Journal of Optoelectronics and Advanced Materials Vol. 6, No. 3, September 2004, p. 1023 - 1028

SIMULATION OF CORONA DISCHARGE IN CONFIGURATIONS WITH A SHARP ELECTRODE

P Atten[a*], K. Adamiak[b], B. Khaddour[a,c], J.-L. Coulomb[c]

[a]Laboratoire d'Electrostatique et de Matériaux Diélectriques, CNRS-Univ. J. Fourier, Grenoble, France
[b]Dept. Electr. & Comp. Engineering, Univ. of Western Ontario, London, Ontario, Canada
[c]Laboratoire d'Electrotechnique Grenoble, INPG/UJF-CNRS, Saint Martin d'Hères, France

Three algorithms are presented to determine the distributions of electric potential and charge density in the case of an injected space charge in a gas. We consider electrode configurations characterised by a sharp electrode injecting charge from the restricted zone where the electric field takes very high values and induces a corona discharge. For the point-plane configuration with a needle having the shape of an axi-symmetric hyperboloid, a change of coordinates transforms the domain of integration into a rectangle, which facilitates the use of finite differences or finite volume methods. For a general axi-symmetric shape of the needle, a finite element method is used to solve the Poisson equation. In these two cases, an adapted method of characteristics makes it possible to solve the charge conservation equation in a way which does not smooth out very high lateral gradients of charge density. In a third approach developed first for the blade-plane electrode configuration, the mesh is redefined with each of the successive approximations. This technique also leads to predictions of current density profile on the plane very similar to the measured ones.

(Received May 26, 2004; accepted July 26, 2004)

*Keywords:*Corona discharge, Electric potential, Charge density

1. Introduction

In many engineering devices and processes using corona discharge in a gas, the injecting electrodes are not wires and the discharges occur in restricted zones of the electrode where the electric field takes high values. In such a case the determination of the field and charge distributions based on a simplified model of the corona discharge are not easy because the boundary condition derived from Kaptzov approximation concerning the field value on the injector cannot be used for electrode shapes other than thin cylinders or spheres [1,2].

We consider here this problem for the typical point-plane and blade-plane configurations. We propose the use of an injection law leading to realistic field values in the injection zone. We also focus on the way to solve the charge conservation equation in order to predict the quasi discontinuities observed in practice.

2. Formulation of the problem

The corona model is simplified by neglecting the thickness of the ionisation layer [2] and considering only one ionic species, moving with a constant mobility. Generally in the papers describing such a model of the corona discharge [1-6], the equations for the electric field (Poisson) and space charge (charge transport) are solved iteratively and many different numerical techniques have been used to obtain the solution. The crucial point concerns the boundary conditions for the space charge density on the corona electrode [1,7].

* Corresponding author: pierre.atten@labs.grenoble.cnrs.fr

2.1 Governing equations

The Poisson equation relates the electric potential V with the charge density ρ:

$$\nabla^2 V = -\frac{\rho}{\varepsilon} \tag{1}$$

where ε is the ambient gas permittivity. V and ρ also satisfy the charge conservation equation, which, when using (1), can be expressed as:

$$E \cdot \nabla \rho = -\frac{\rho^2}{\varepsilon} \qquad \text{with} \qquad E = -\nabla V \tag{2}$$

Eq. (2) is valid under the assumptions that *i*) the medium conductivity is zero, *ii*) the ions diffusion is negligible and their mobility is constant *iii*) the convection velocity is much lower than the drift velocity of charge carriers.

2.2 Boundary conditions

The corona (Γ_{inj}) and ground (Γ_{coll}) electrodes are equipotential, which leads to:

$$V = V_{appl} \qquad \text{on} \qquad \Gamma_{inj}, \qquad V = 0 \quad \text{on} \qquad \Gamma_{coll} \tag{3}$$

Only one boundary condition is associated with $\rangle$; from the mathematical viewpoint the charge density must be given on the injector Γ_{inj} [7]. Physically the corona discharge depends on the field strength and a way to retain this decisive dependence is to prescribe an injection law ρ = f(E) depending on the field value at the considered point on the corona electrode. The simplest injection law is:

$$\rho = \alpha(E - E_s) \quad \text{for} \quad E > E_s \tag{4}$$

where α is a constant and E_s is the local field value corresponding to the local corona onset. In practice, retaining very large values for α leads to a generalisation of Kaptzov condition [8] (the threshold field can be defined from Peek's law [9] with the local curvature of the electrode). By taking appropriate references for the different variables, the problem is, in non dimensional form:

$$\nabla^2 V = -\rho \tag{5}$$

$$E \cdot \nabla(1/\rho) = 1 \qquad \text{with} \qquad E = -\nabla V \tag{6}$$

with the boundary conditions:

$$V(P) = 1, \qquad \rho(P) = A[E(P) - E_s(P)] \quad (E > E_s) \qquad P \in \Gamma_{inj} \tag{7}$$

$$V(P) = 0, \qquad P \in \Gamma_{coll} \tag{8}$$

3. Change of variables for hyperbolic needle – plate configuration

Assuming an axisymmetric needle of hyperbolic shape, it is possible to treat the problem by using hyperboloidal coordinates defined by:

$$\begin{cases} x = c \sinh\xi \quad \cos\theta \cos\varphi \\ y = c \sinh\xi \quad \cos\theta \cos\varphi \\ z = c \cos\xi \quad \sin\theta \end{cases} \tag{9}$$

where $c = (1+R)^{1/2}$, R being the radius of curvature at the needle tip. The interest of this change of variables is to transform the domain of integration between the needle (tip at z = -1) and the plate

(z = 0) into a rectangle, which facilitates the use of finite difference methods to solve the two equations which write, in $\theta - \xi$ coordinates:

$$\frac{\partial}{\partial\theta}\left(\sinh\xi\cos\theta\frac{\partial V}{\partial\theta}\right)+\frac{\partial}{\partial\xi}\left(\sinh\xi\cos\theta\frac{\partial V}{\partial\xi}\right)=-c^2\sinh\xi\cos\theta\left(\sinh^2\xi+\cos^2\theta\right)\rho \tag{10}$$

$$\frac{\partial V}{\partial\theta}\frac{\partial}{\partial\theta}\left(\frac{1}{\rho}\right)+\frac{\partial V}{\partial\xi}\frac{\partial}{\partial\xi}\left(\frac{1}{\rho}\right)=-c^2\left(\sinh^2\xi+\cos^2\theta\right) \tag{11}$$

Defining a rectangular mesh, the Poisson equation (10) is converted into classical finite difference equations solved by the over-relaxation technique for a given space charge distribution. For a given potential distribution, (11) is a first order equation which can be solved by the method of characteristics (MOC). The local treatment on the elementary rectangles of the mesh leads to a rather important numerical diffusion which prevents to obtain steep charge density gradients as observed experimentally. This method has been adapted to lead to better predictions: from each node of the mesh the characteristic line is determined upwards to the injecting needle; at the intersection point the injected charge density is calculated from the condition (7) and the ρ value at the node is then derived through a simple analytic expression.

Taking the harmonic potential as the starting V distribution, the solution is determined by successive approximations (an under-relaxation technique is necessary to obtain convergence of the iterative process and particular care has been devoted to the practical use of the injection law). Fig. 1 shows a charge distribution in the $\theta - \xi$ plane. In this plane the harmonic field lines are vertical segments and it is clear that there is a very marked influence of the injected space charge on the spreading of the field lines (this case corresponds to an applied voltage 3 times greater than the corona discharge inception voltage V_s). This figure also exhibits the very steep gradient in ρ with the existence of a separatrix between the charged and the charge free zones. This quasi-discontinuity is also visible on the radial distribution of current density j on the plate $z = 0$ (Fig. 2). Note that the drop of j occurs at a radius grossly equal to the needle-plate distance.

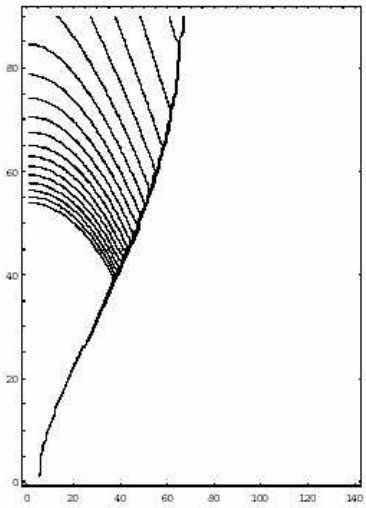

Fig. 1. Equi-charge density lines in θ - ξ plane (the horizontal lines $\xi = 0$, ξ 2.05 represent the injecting and collecting electrodes). Hyperbolic needle of radius of curvature R =0.005, $V_{appl} = 3\ V_s$ (90 × 140 nodes).

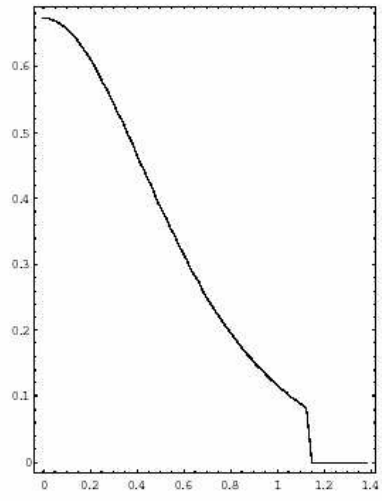

Fig. 2. Current density profile on the plate $z = 0$ facing the needle as a function of the distance from the axis $x = y = 0$. Hyperbolic needle of radius of curvature $R = 0.005$, $V_{appl} = 3\ V_s$ (90 ×140 nodes).

The distribution of electric field along the axis, from needle tip to the plate, is shown in Fig. 3 (in this figure the field has been non dimensionalised with respect to the threshold voltage V_s). It can be seen that the field departs from the harmonic field values above some distance from the needle which decreases as the space charge and applied voltage increase.

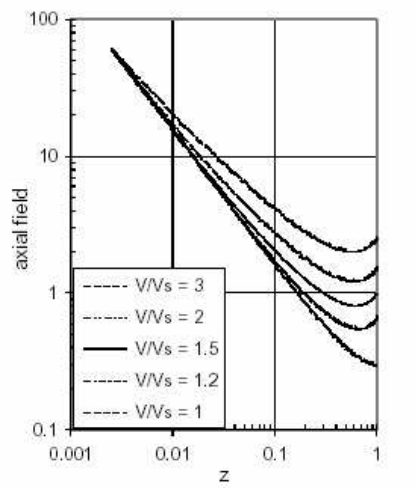

Fig. 3. Variations of the electric field E_z along the axis of symmetry Oz for various values of the applied voltage. Hyperbolic needle of radius of curvature $R = 0.005$, (90×140 nodes).

4. Numerical technique for a needle of any shape

For a non hyperbolic shape of the needle, the change of variables (9) gives a domain in the θ - ξ plane which is not simply a rectangle; this would result in rather intricate expressions when retaining the finite difference method. A more general approach [10] has been developed, based on three numerical techniques: the Boundary Element Method (BEM), the Finite Element Method (FEM) and the Method of Characteristics (MOC). A hybrid BEM-FEM technique is used to determine the electric potential satisfying (5): the solution of the Laplace equation is obtained by the BEM and a structured mesh is defined from the corresponding equipotential and field lines; then the modification of the electric potential associated with the space charge is determined by the FEM [10]. Once the new field distribution is obtained, the MOC is used to solve equation (6); in practice the charge density ρ is determined on the injector and then along a series of field lines issuing from the needle electrode and the ρ values at the nodes are obtained from interpolation [10]. Both problems associated with eqs. (5) and (6) are solved iteratively until the convergence is reached for all involved variables : potential V, space charge density ρ and charge density $\rho_s(P)$ on the electrode surface.

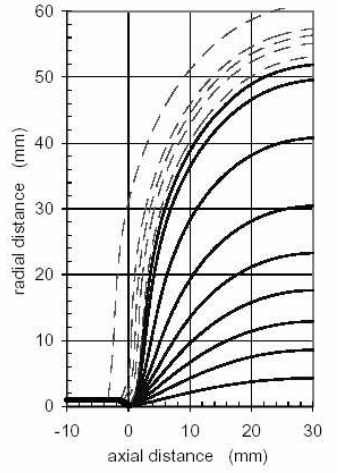

Fig. 4. Field lines in the charged and the charge Free zones. Cylinder ($\phi = 2$ mm) and cone Needle with a spherical cap of radius R =100 µm, distance d = 30 mm, V_{appl} = 15 kV.

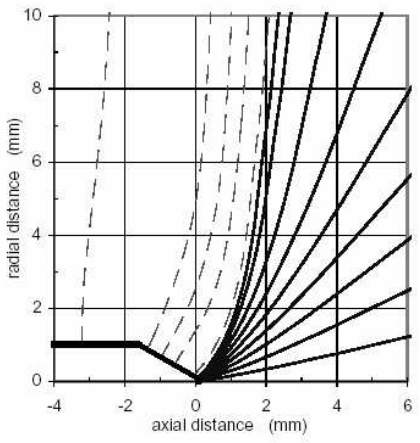

Fig. 5 – Magnified view around the needle tip of the field lines showing that the charge injection emanates from a part of the spherical cap (same solution as in fig. 4).

The Figs. 4 to 7 exhibit some results obtained for a practical set-up using a needle with a conical end smoothed by a spherical cap having a radius of 100 µm. Figs. 4 and 5 give the shape of the field lines : beyond a first zone with grossly radial field lines, the strong space charge induces a marked divergence of the field lines which spread out; the separatrix between the charged and charge free zones reaches the plate at distance from the axis nearly two times the needle-plate distance. By taking the classical Peek's formula for the field value of corona discharge threshold and applying relation (4) with very large α values, the current density j on the grounded plate is fairly well predicted (Figs. 6 and 7). In particular the predicted radius of the space charge zone (where j drops to zero) is close of the measured one (see also [10]).

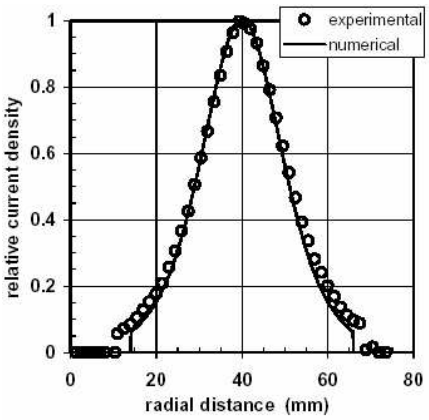

Fig. 6. Current density profile on the plate facing the needle as a function of the distance from axis (R = 20 µm, d = 20 mm, V_{appl} = 8 kV).

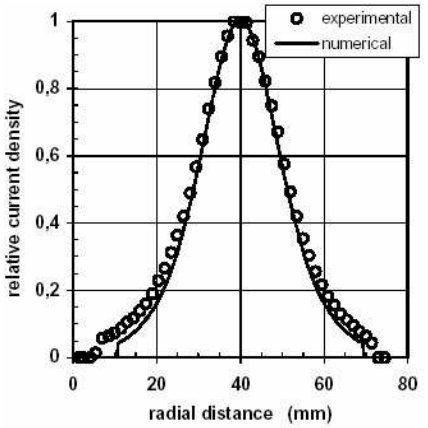

Fig. 7. Current density profile on the plate facing the needle as a function of the distance from axis (R = 20 µm, d = 20 mm, V_{appl} = 10 kV).

5. Mesh redefinition technique

In sections 3 and 4, particular ways of solving the charge equation (6) have been used in order to avoid the numerical diffusion existing when solving the first order equation (6) with a fixed mesh (the ρ distribution then does not exhibit the quasi-discontinuity revealed by Figs. 2, 6 and 7). Another technique suggested for the space charge problems [11] consists in redefining the structured mesh at each iteration step. Here we define the new nodes as intersections of the field and equi-potential lines of the new approximation of the potential. The nodes on the field lines are defined by predetermined values of the potential. In this way, (6) is easily (and rapidly) integrated along the characteristics (the finite volume method can also been used to obtain ρ).

As in section 4, at the iteration step #k, the finite element method is used to solve the Poisson equation and the potential is obtained at the nodes of the structured mesh #(k-1). The field lines are determined not directly from the piecewise linear approximation of V but from local linear approximations of the potential by least squares method applied to the 6 nodal values of two neighbouring quadrangles. This method is sensitive to the space charge. For high values of the injected charge density, if the nodes on the injecting electrode are not redefined, after some iterations the field lines exhibit a strong divergence in the charged zone (Fig. 8) and the computation fails (numerical instability).

To obtain a more regular mesh, it is necessary to redefine the nodes position on the injecting electrode. This is done through relations involving the nodes separations on the plane (where the electrical lines arrive) at step #(k-1) and predetermined separations. Furthermore an under-relaxation process is used to damp out oscillations of successive occurrences of the mesh.

With this technique we build a new structured mesh after each new determination of the potential until convergence of the iteration process. Several distributions of predetermined potential values and nodes separations on the plane were tested in order to obtain a regular enough mesh with fine distribution of nodes in the zones of strong field and charge density.

By adequately choosing the various parameters influencing the rate of convergence, we obtained good convergence of the algorithm for the 2-D blade-plane configuration (the mean relative difference between two successive approximations of the charge density distribution becomes lower than 10^{-4} after 40 to 50 iterations for a 50×50 mesh). The MOC technique with redefinition of the mesh gives very satisfactory results : the current flowing from the blade to the plate is conserved (fluctuations ~ 10^{-3}). In the case of a rectangular distribution for ρ_{inj}, there is no diffusion of charge across the field line separating the charged and charge free zones and Fig. 9 clearly shows the sudden drop of current density on the collecting plate.

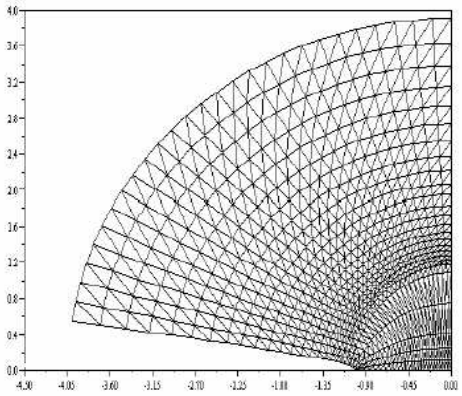

Fig. 8 . Mesh deformation after several iterations for fixed nodes on the injecting electrode (blade of hyperbolic cross-section, radius of curvature R = 0.02).

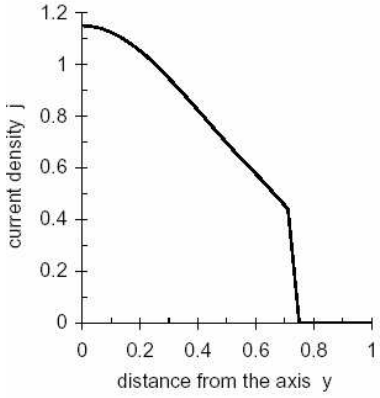

Fig. 9. Current density profile on the plane for a blade of hyperbolic cross - section (R = 0.02). Rectangular distribution of charge density ρ_{inj} on the blade (ρ_{max} = 15, 31×31 mesh).

6. Conclusions

The technique of mesh redefinition is very well suited for the problem of electric field modified by an injected space charge. It has two noticeable advantages: i) the resolution of the charge conservation equation is very straightforward; ii) the mesh immediately gives the equipotential curves and the field lines. This approach is under development and should give the solution involving the injection law as expressed by (4). The resolution by successive approximations should be very similar to the one used in the two other algorithms (§3 and §4).

Last but not least, the mesh redefinition approach should be extended to three-dimensional configurations without major difficulty and without marked changes.

References

[1] K. Adamiak, P. Atten, Actes du congrès S.F.E. 2002, Congrès 2002 de la Société Française d'Electrostatique, Toulouse, 3-4 juillet 2002, 8 pages (CD-ROM).
[2] P. Atten, K. Adamiak, V. Atrazhev, 2002 Annual Report, Conference on Electrical Insulation and Dielectric Phenomena, Cancun, Mexico, pp. 109-112, October 2002.
[3] J. R. McDonald, W. B. Smith, H. W. Spencer III, L. E. Sparks, J. Appl. Phys. **48**, 2231 (1977).
[4] S. Cristina, G. Dinelli, M. Feliziani, IEEE Trans. on Ind. Appl. **27**, 147 (1991).
[5] J. L. Davis, J. F. Hoburg, J. Electrostatics **14**, 187 (1983).
[6] P. L. Levin, J. F. Hoburg, IEEE Trans. Ind. Appl. **IA26**, 662 (1990).
[7] P. Atten, Revue Gén. Electr. **83**, 143 (1974).
[8] N. A. Kaptzov, Elektricheskiye Yavleniya v Gazakh i Vacuume. Moscow: OGIZ, 1947.
[9] A. M. Meroth, T. Gerber, C. D. Munz, P. L. Levin, A. J. Schwab, J. Electrostatics **45**, 177 (1999).
[10] K. Adamiak, P. Atten, J. Electrostatics **61**, 85 (2004).
[11] M. Abdel-Salam, Z. Al-Hamouz, J. Phys. D: Appl. Phys. **26**, 2202 (1993).